Universiteit
Leiden
The Netherlands

Unraveling mechanisms of vascular remodeling in arteriovenous fistulas for hemodialysis

Wong, C.Y.

Citation
Wong, C. Y. (2017, March 8). *Unraveling mechanisms of vascular remodeling in arteriovenous fistulas for hemodialysis*. Retrieved from https://hdl.handle.net/1887/46406

Version:	Not Applicable (or Unknown)
License:	Licence agreement concerning inclusion of doctoral thesis in the Institutional Repository of the University of Leiden
Downloaded from:	https://hdl.handle.net/1887/46406

Note: To cite this publication please use the final published version (if applicable).

Cover Page

Universiteit Leiden

The handle http://hdl.handle.net/1887/46406 holds various files of this Leiden University dissertation.

Author: Wong, C.Y.
Title: Unraveling mechanisms of vascular remodeling in arteriovenous fistulas for hemodialysis
Issue Date: 2017-03-08

Chapter 5

Elastin is a key regulator of outward remodeling in arteriovenous fistulas

C.Y. Wong, T.C. Rothuizen, M.R. de Vries, T.J. Rabelink, J.F. Hamming, A.J. van Zonneveld, P.H.A Quax and J.I. Rotmans

Eur J Vasc Endovasc Surg. 2015 Apr;49(4):480-6

Introduction

An adequate functioning arteriovenous fistula (AVF) is of the preferred type of vascular access for patients requiring chronic hemodialysis. AVF maturation (e.g. increase in flow and venous diameter) is a prerequisite for successful cannulation of the venous outflow tract. Unfortunately, 30-50% of fistulae fail to mature[1] eventually leading to a poor one-year primary patency of 60-65%[2, 3]. The pathophysiology responsible for inadequate maturation is incompletely understood.

AVF maturation results from a cascade of processes after AVF surgery that leads to the reorganization of the extracellular matrix (ECM)[4]. This matrix-metalloproteinase (MMP)-mediated process of vascular remodeling allows the vessels of the fistula to enlarge. The main ECM components that are involved in this outward remodeling (OR) are collagen and elastin. In vascular physiology, elastic fibers provide the vessel its elasticity and resilience, thereby providing the ability to absorb hemodynamic stress[5, 6]. Elastin is a cross-linked, insoluble polymer of the monomeric secreted form of the protein tropoelastin that is secreted primarily by vascular smooth muscle cells (VSMCs) and diverse fibroblasts[6, 7]. Elastin homeostasis has emerged as an important determinant of vascular OR. Indeed, elastic fiber degradation mediates physiological OR as occurs in the uterine artery during pregnancy[8, 9]. Additional support for a role of elastin degradation in OR comes from studies in patients with aortic aneurysms showing that polymorphisms in the elastin gene[10] may contribute to the pathogenesis of this pathological arterial dilation. In the present study, we hypothesized that elastin might be an important regulator in outward remodeling in AVF. For this purpose, end-to-side AVFs were created in haplodeficient tropoelastin KO mice[11].

Material and Methods

Animals and study design

The Institutional Committee for Animal Welfare at the LUMC approved all experiments. Adult male C57BL/6 (WT) (Charles River) and $eln^{+/-}$ mice with a C57BL/6 background aged 10-17 weeks (weighing 23-35 grams) were used for the experiments and received unilateral AVFs. The animals were sacrificed at day 21 after the surgical procedure. Identical veins of unoperated mice were used to assess elastic fiber density before surgery.

Surgical procedure

An unilateral AVF was created as previously described[12] (Fig 1, A). In short, the animal was anesthetized using isoflurane followed by shaving and disinfection of the skin in the ventral neck area and fixed in a supine position on a heating blanket. The mouse was then injected with buprenorphin (0.1 mg/kg) (MSD, Whitehouse Station, NJ, USA) and 0.5 mL saline. Under a dissecting microscope (M80, Leica, Wetzlar, Germany), an incision in the ventral midline of the neck area was made, followed by a dissection of the right dorsomedial branch of the external jugular vein and ipsilateral common carotid artery after the excision of the sternocleidomastoid muscle using a heat cauterizer. Next, after applying a vascular clamp (S&T, Neuhausen, Switzerland) on the proximal and distal artery an approximate 1 mm incision was made using a microscissor (Fine Science Tools, Heidelberg, Germany) and the lumen was rinsed with a heparin solution (100 IU/mL) (LEO Pharma, Ballerup, Denmark). The vein was then clamped proximally and ligated distally, followed by a transsection just proximal to the ligation. After rinsing the vein with a heparin solution, an end-to-side anastomosis was created using 10.0 interrupted sutures (BBraun, Melsungen, Germany). Halfway during the suturing procedure heparin was injected intravenously with a dose of 0.2 IU/gram bodyweight. After completion of the anastomosis, the remaining clamps were removed and patency was assessed. The skin was closed with a 6.0 running suture suture (BBraun, Melsungen, Germany). Following completion of the surgery 0.5 mL of saline was injected subcutaneously and the animals were kept warm until recovery.

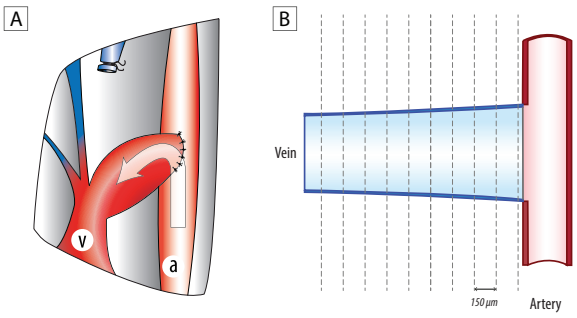

Figure 1. Surgical scheme and orientation of sectioning. (A) Schematic visualization of an arterial side to venous end arteriovenous anastomosis between the common carotid artery (a) and the dorsomedial distal branch of the external jugular vein (v) using 10.0 interrupted sutures. (B) Schematic overview of sectioning locations within the arteriovenous fistula, in which every dashed line represents a sectioning area with a fixed interval of approximately 150 µm.

Tissue harvesting and processing

Upon sacrifice, animals received an intraperitoneal injection with an anesthetic-mixture containing midazolam (5 mg/kg) (Roche, Basel, Switzerland), medetomidine (0.5 mg/kg) (Orion, Espoo, Finland) and fentanyl (0.05 mg/kg) (Janssen, High Wycombe, UK) whereupon a reincision was made over the scar. The AVF, including its venous and arterial limb, was dissected and the patency was assessed clinically. For this purpose, the blood flow was disrupted by compressing the distal arterial as well as the distal venous limb with vascular forceps. The AVF was considered patent when the venous limb proximal to the forceps expands in diameter. In case this phenomenon was not clearly visible, the AVF was considered not patent. Next, a thoracotomy was performed and the inferior vena cava was transected followed by an intracardial perfusion with subsequently phosphate buffered saline and formalin 4% at a pressure of approximately 100 mmHg. The small size of the murine vasculature and the configuration of the AVF preclude simultaneous perpendicular analysis of the artery and the vein. Since most of the stenotic lesions in human AVFs occur in the venous outflow tract, we focused our analysis on the vein. (Fig 1, B) The tissue was processed to paraffin and sections of 5 μm were made perpendicular to the vein at 12 locations with an interval of 150 μm. For the purpose of RNA isolation, 20 μm thick sections were obtained from additional animals.

RNA islolation and real-time quantitative polymerase chain reaction (RT-QPCR)

Twenty paraffin embedded sections section of 20 μm-thick representing the entire AVF were freshly collected and RNA was isolated from the tissue using RNeasy FFPE Kit (Qiagen, Gaitherburg, Maryland, USA). RNA concentration, purity and integrity were examined by nanodrop (Nanodrop® Technologies). Relative quantitative mRNA PCR was performed on reverse transcribed cDNA (High Capacity RNA-to-cDNA kit - Applied Biosystems art.nr. 4387406) using primers against mouse eln (Mm00514670_m1, Life technologies, Grand Island, New York, USA). qPCRs were run on a 7900HT Fast Real-Time PCR System (Applied Biosystems). Normalization of data was performed using stably expressed endogenous controls (HPRT).

Spectral microscopy

To study the dispersion of elastic fibers in more detail, sections stained with Weigert's elastin were analyzed using multispectral imaging system comprised of a fluorescent microscope (DM4000B, Leica, Wetzlar) and a Nuance imaging unit (N-MSI-FX, PerkinElmer, Massachusetts, USA). In short, the specific spectrum of elastin was selected using the elastic lamellae present in the carotid artery. This tissue specific selection was then located in the venous outflow tract of the AVF and assigned the color red. The background was assigned the color green.

Morphometric analysis

A histochemical staining with hematoxylin, phloxin and saffron (HPS) was used for a morphological overview. After digitalization of all the venous sections with a microscope (Carl Zeiss, Oberkochen, Germany), morphometric analysis was performed on Weigert's elastin stained sections using quantitative imaging software (Qwin, Leica, Wetzlar, Germany). The intimal area was calculated by subtracting the luminal area from the area within the internal elastic lamina (IEL). The circumference of the vessel was determined by measuring the length of the IEL. Results are expressed as mean ± standard error of the mean.

Alpha smooth muscle actin staining and quantification

All sections were stained against α-smooth muscle actin (α-sma) to identify vascular smooth muscle cells (VSMC) and myofibroblasts using a dilution of 1:1000 for the primary antibody (Dako, Glostrup, Denmark). Subsequently, the slides were digitized at a resolution of 2080 x 1542 pixels by a camera connected to a microscope (Carl Zeiss, Oberkochen, Germany). A detailed protocol of the staining is listed in the appendix. The α-sma positive area in the total vessel was measured using quantitative imaging software (ImageJ) and was expressed in μm^2.

Collagen quantification

In order to quantify the collagen content in the vessels, the tissue sections were first stained using a picro-sirius red staining and followed by digitalization using the method as described above. Using ImageJ software, collagen content in all the venous sections was determined by selecting the stain specific color for collagen at a fixed average threshold12, and was expressed in μm2. In order to obtain qualitative information about the deposition pattern of collagen additional images were produced using digital image microscopy with circularly polarized light (Olympus, Shinjuku-ku, Tokyo, Japan.).

Statistical analysis

All data except the patency outcome were expressed as mean ± standard error of the mean. A Fisher's exact test was used for the data on AVF patency. For the histomorphometric and RT-QPCR results an unpaired t-test was used. The results from the α-sma quantification were tested using a Mann-Whitney U test. A P-value < 0.05 was considered statistically significant.

Results

Surgical outcome

Twenty animals (11 WT mice and 9 eln$^{+/-}$ mice) successfully received an AVF out of which 2 (18%) from the WT group and 1 (11%) from the eln+/- group were occluded 21 days after surgery (P = 1.0). No difficulties were encountered during the surgical procedure in the eln$^{+/-}$ mice. These occluded AVFs were excluded from morphometric analysis, resulting in an inclusion of 9 WT mice and 8 eln$^{+/-}$ mice.

Elastin expression

At the mRNA level, a relative reduction of 53% in expression of the mELN gene in eln$^{+/-}$ mice was observed as compared to the WT mice (1.0 ± 0.19 vs 0.47 ± 0.07, P < 0.001) (Fig 2, *A*). Using spectral microscopy, we observed a reduction in elastin accumulation in the IEL of eln$^{+/-}$ mice before AVF placement, resulting in a more fragmented IEL structure (Fig 2, B-*E*). After 21 days of venous arterialization, elastin content in the vessel wall is greatly fragmented and diminished in both the WT (n=5) and eln$^{+/-}$ mice (n=6), retaining the pre-existing difference in elastin content favouring the WT group.

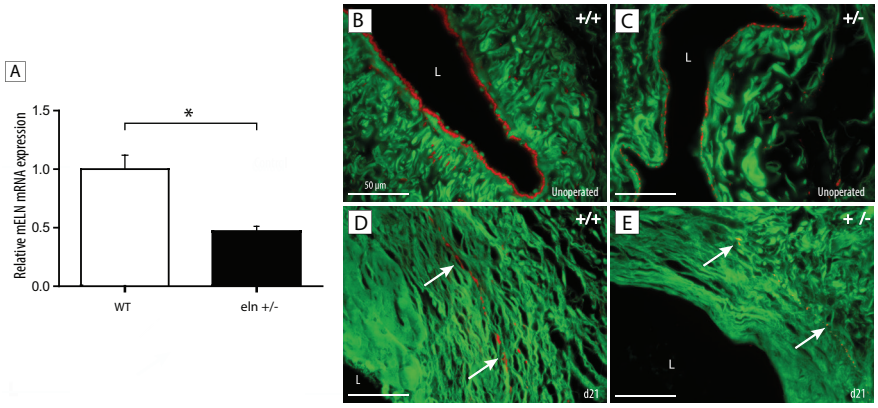

Figure 2. The presence of elastin in the venous outflow tract prior to, and after arteriovenous fistula creation. (A) Relative mRNA expression of murine elastin in the AVF at day 21 after surgery. (B–E) Visualization of elastin (red) (white arrow) in the venous outflow tract before (control) and after surgery (day 21) using spectral microscopy. *Note*. Original magnification 100×. Scale bar, 50 µm; L = Lumen; +/+ = wild type; +/− = haplodeficient. *$p < .05$.

Morphometric analysis

Twenty one days after AVF placement, the circumference in eln$^{+/-}$ mice (2936 ± 191 μm) was 21% larger as compared to the WT mice (2424 ± 126 μm; P = 0.037), whereas the intimal area was comparable between the groups (WT: 112908 ± 16029 μm^2 vs eln$^{+/-}$:134967 ± 24673 μm^2;P = 0.45). The luminal area of the venous outflow tract in the eln$^{+/-}$ mice was 53% larger as compared to the WT mice, although this difference was borderline significant (eln$^{+/-}$: 350116 ± 45073 μm^2, WT: 229405 ± 40453 μm^2; P = 0.064). (Fig 3, *A-F*).

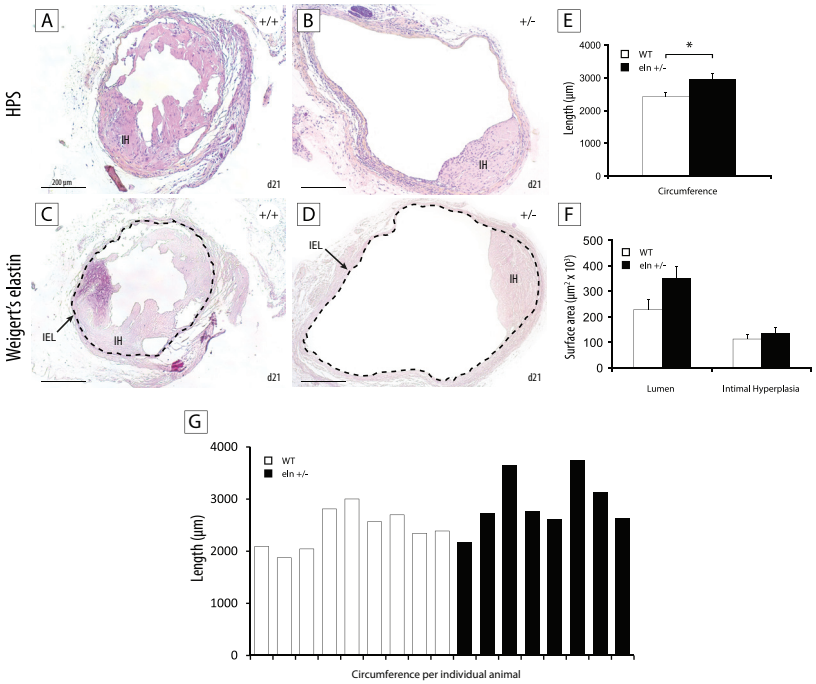

Figure 3. Morphometric parameters 21 days after AVF creation. (A,B) Hematoxylin, phloxin, and saffron staining (HPS). (C,D) Weigert's elastin staining used for the histomorphometric analysis in which the internal elastic lamina (IEL) is highlighted (dashed line). (E,F) Histomorphometric data after AVF creation. (G) Mean circumference displayed per individual animal. Original magnification 100×. Scale bar, 200 μm. IH = intimal hyperplasia. * $p < .05$.

Alpha smooth muscle actin

Although the amount of intimal hyperplasia was equal in both groups after 21 days, we did observe an 2.4 fold larger area of α-sma positive cells in the venous outflow tract of the haplodeficient mice as compared to the WT (132169 ± 30725 μm^2 vs 55331 ± 8053 μm^2; P = 0 .036) (Fig 4, *A-C*).

Collagen

At day 21, the amount of collagen observed in the eln$^{+/-}$ mice (129539 ± 19246 μm^2) was 87 % higher as compared to the WT mice (69180 ± 11574 μm^2, P = 0.015). (Fig 4, *D-F*). The pico-sirius red stained sections, analyzed with circularly polarized light revealed that collagen type I and III was mainly located in the media and adventitia, with limited collagen content in the intima.

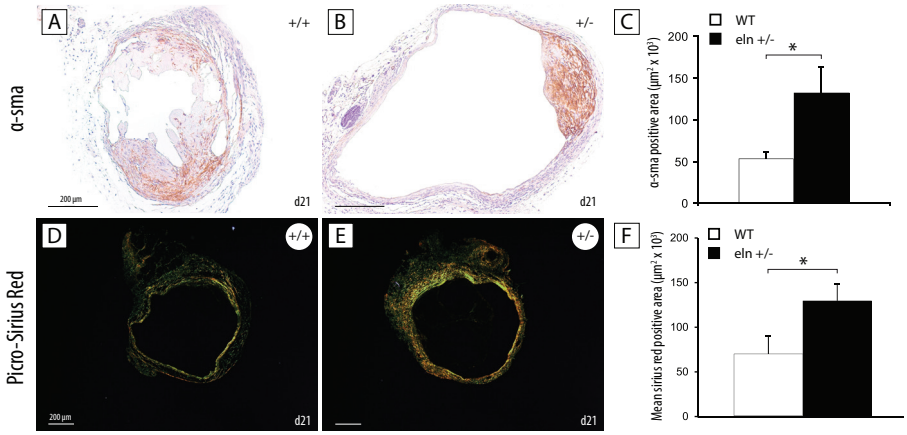

Figure 4. Alpha smooth muscle actin and picro-sirius red staining. (A,B) Immunohistochemical staining using antibodies against α-sma. (C) Quantification of α-sma positive area in the venous outflow tract. (D,E) Picro-sirius red staining visualized using circular polarized light microscopy. (Original magnification 40×). (F) Quantification of collagen positive area using the picro-sirius red staining. Original magnification 100×. Scale bar, 200 μm. * $p < 0.05$.

Discussion

In the present study we investigated the effect of elastin deficiency on venous remodeling in a murine model of AVF failure. We observed that eln+/- mice have a lower density of elastic fibers present in the venous IEL prior to AVF creation when compared to WT mice. Upon AVF creation, $eln^{+/-}$ mice showed an accelerated venous outward remodeling response while no effect was observed on intimal hyperplasia. This adaptive response in the $eln^{+/-}$ mice resulted in a trend towards a larger luminal area of the venous outflow tract when compared to WT mice.

The role of elastin in outward remodeling after arteriovenous fistula creation

The main objective of AVF surgery in hemodialysis patients is to create a high-flow vascular circuit with a sufficient venous intraluminal diameter to allow safe cannulation. According to the KDOQI guidelines, AVF maturation is considered clinically successful if 6 weeks after surgery, the fistula supports a flow of 600 mL/min, is located at a maximum of 6 mm from the surface and has a diameter of > 6 mm[13]. In order to achieve the latter, adequate outward remodeling of the venous outflow tract is required. The data from the present study in which we observed enlarged OR in the elastin haplodeficient mice provides support for the hypothesis that a low elastin content in the venous outflow tract might facilitate AVF maturation. In addition, a reduced elastin expression in the carotid artery might also have contributed to the increase in venous outward remodeling since increased arterial outward remodeling could stimulate flow-induced venous remodeling. Unfortunately, the end-to-side configuration of the AVF precluded morphometric analysis of cross-sections of the arterial segment. Since intimal hyperplastic lesions in AVF mostly occur in the venous outflow tract, we chose to focus on this segment by cross-sectioning the venous part.

Previous clinical studies have also suggested that elastin degradation might be beneficial for AVF maturation by showing that patients with matured AVF have higher circulating levels of MMP 2 (an elastinolytic protease), when compared to those with maturation failure[14]. A similar association has been observed between high MMP-2 expression in venous segments of AVFs and maturation of these fistulas[15]. Conversely, peri-adventitial application of recombinant elastase has been shown to stimulate OR in rabbit AVF[16]. Interestingly, this approach has recently been investigated in a phase II clinical trial that revealed increased maturation of radiocephalic fistulas that were treated with 30 μg elastase[17].

The role of collagen in AVF adaptation is more complex since MMPs are not only involved in collagen degradation, but they also induce collagen synthesis[18]. The higher amount of total collagen observed in the $eln^{+/-}$ mice corresponds with the larger vessel wall area as compared to the WT mice. Indeed, newly synthesized collagen fibers are required in order to keep in

pace with the growing dimensions of the venous vessel wall. Most likely, VSMCs are the major source of collagen since during vascular remodelling, proliferating VSMCs synthesize large amounts of collagen[19].

Intimal hyperplasia in elastin haplodeficient mice

In our study, we did not observe a significant difference in intimal hyperplasia (IH) between the eln $^{+/-}$ and WT mice 21 days after surgery. Obviously, increased IH might be the downside of impaired elastin synthesis since elastin is an important inhibitor of VSMC migration and proliferation[20-22] one of the main mechanisms underlying the development of IH[23]. The importance of elastin in vascular function and integrity becomes clear, as homozygous knock-out mice are not viable due to the formation of occlusive arterial lesions consisting of VSMCs[24]. In line, increased activity of MMP-2 and MMP-9, have also been associated with IH in arteriovenous conduits[25-27]. In the previous studies in the murine AVF model, we observed progressive growth of intimal hyperplastic lesions up to 4 weeks after surgery[12]. In view of the inhibitory effect of elastin on VSMC proliferation, we cannot exclude that elastin deficiency might result in enhanced IH at later time points after surgery.

Interestingly, Franano and coworkers observed an 84% reduction in intimal area in the outflow vein of an rabbit AVF after perivascular application of porcine elastase[28]. This beneficial effect on IH is most likely driven by the perivascular delivery method of elastase resulting in a directional VSMC proliferation and migration to the adventitia rather than the intima[29, 30]. This location specific elastolytic process, however, is absent in our used model as we only study the effect of impaired elastin synthesis that does not specifically target the adventitia.

While the size of the intimal area did not differ between the WT en eln$^{+\backslash -}$ mice, we did observe a larger content of α-sma positive cells in the venous outflow tract of the eln$^{+/-}$ mice. The latter results from a higher density of α-sma positive cells in the intima. In addition, the enhanced OR response in eln$^{+/-}$ mice also resulted in a larger VSMCs content in the adventitia and media. This observation supports the hypothesis that VSMC proliferation in the initial phase after AVF surgery is required in order to keep pace with the expansion of the venous outflow tract, as demonstrated previously in flow induced arterial OR in rats[31].

Study limitations

The uremic milieu has a clear impact on the progression of vascular diseases in end-stage renal disease patients. Recent studies have suggested that uremic conditions also contribute to the formation of IH in veins prior to AVF surgery[32, 33]. In order to further elucidate the mechanisms involved in AVF maturation, the incorporation of chronic renal failure[34] would be of added value.

Another limitation of our experiments is the absence of data on flow measurements since a high blood flow is one of the main characteristics of a functional AVF for hemodialysis access. Due to technical reasons, quantification of blood flow using ultrasonography or MRI was not successful in our hands.

Although murine models are useful to study the pathophysiology of human diseases, we should remain cautious in the extrapolation of these results to the human setting because the pathology in animals does not necessarily mimic the pathology in humans.

Finally, we should take into account that we could not incorporate the homozygous $eln^{-/-}$ mouse into our AVF model, due to its lethal phenotype. Nevertheless, we think the haplodeficient mice still provide a good indication of the vascular remodeling process in elastin deficient blood vessels.

In conclusion, in the present study we showed that elastin is a crucial factor in OR in murine AVF. This study provides further evidence that interventions aimed at the promotion of elastin degradation such as local application of elastase could be a viable option to enhance maturation of AVFs.

Acknowledgements

This study was supported by a grant from the Dutch Kidney Foundation (KJPB 08.0003). We would like to thank Erna Peters and Iris Schmidt for their assistance on the RT-QPCR and pathology work-up. The knockout mice were generated at the University of Utah by Dr. Dean Li and coworkers. We thank him as well as Dr. Hiromi Yanagisawa from Southwestern Medical Center, Dallas, Texas for providing the elastin haplodeficient mice.

Reference List

1. Tordoir JH, Rooyens P, Dammers R, van der Sande FM, de HM, Yo TI. Prospective evaluation of failure modes in autogenous radiocephalic wrist access for haemodialysis. Nephrol Dial Transplant 2003 Feb;18(2):378-83.

2. Falk A. Maintenance and salvage of arteriovenous fistulas. J Vasc Interv Radiol 2006 May;17(5):807-13.

3. Dixon BS, Novak L, Fangman J. Hemodialysis vascular access survival: upper-arm native arteriovenous fistula. Am J Kidney Dis 2002 Jan;39(1):92-101.

4. Rothuizen TC, Wong C, Quax PH, van Zonneveld AJ, Rabelink TJ, Rotmans JI. Arteriovenous access failure: more than just intimal hyperplasia? Nephrol Dial Transplant 2013 May;28(5):1085-92.

5. Li DY, Faury G, Taylor DG, Davis EC, Boyle WA, Mecham RP, et al. Novel arterial pathology in mice and humans hemizygous for elastin. J Clin Invest 1998 Nov 15;102(10):1783-7.

6. Wise SG, Weiss AS. Tropoelastin. Int J Biochem Cell Biol 2009 Mar;41(3):494-7.

7. Wagenseil JE, Mecham RP. New insights into elastic fiber assembly. Birth Defects Res C Embryo Today 2007 Dec;81(4):229-40.

8. Harris LK, Aplin JD. Vascular remodeling and extracellular matrix breakdown in the uterine spiral arteries during pregnancy. Reprod Sci 2007 Dec;14(8 Suppl):28-34.

9. Harris LK, Smith SD, Keogh RJ, Jones RL, Baker PN, Knofler M, et al. Trophoblast- and vascular smooth muscle cell-derived MMP-12 mediates elastolysis during uterine spiral artery remodeling. Am J Pathol 2010 Oct;177(4):2103-15.

10. Saracini C, Bolli P, Sticchi E, Pratesi G, Pulli R, Sofi F, et al. Polymorphisms of genes involved in extracellular matrix remodeling and abdominal aortic aneurysm. J Vasc Surg 2012 Jan;55(1):171-9.

11. Li DY, Faury G, Taylor DG, Davis EC, Boyle WA, Mecham RP, et al. Novel arterial pathology in mice and humans hemizygous for elastin. J Clin Invest 1998 Nov 15;102(10):1783-7.

12. Wong CY, de Vries MR, Wang Y, van der Vorst JR, Vahrmeijer AL, van Zonneveld AJ, et al. Vascular remodeling and intimal hyperplasia in a novel murine model of arteriovenous fistula failure. J Vasc Surg 2013 May 15.

13. Clinical practice guidelines for vascular access. Am J Kidney Dis 2006 Jul;48 Suppl 1:S248-S273.

14. Lee ES, Shen Q, Pitts RL, Guo M, Wu MH, Sun SC, et al. Serum metalloproteinases MMP-2, MMP-9, and metalloproteinase tissue inhibitors in patients are associated with arteriovenous fistula maturation. J Vasc Surg 2011 Aug;54(2):454-9.

15. Lee ES, Shen Q, Pitts RL, Guo M, Wu MH, Yuan SY. Vein tissue expression of matrix metalloproteinase as biomarker for hemodialysis arteriovenous fistula maturation. Vasc Endovascular Surg 2010 Nov;44(8):674-9.

16. Burke SK, Franano FN, Mendenhall V, Howk K, LaRochelle A, Wong M, et al. Recombinant human elastase (PRT-201) dilates outflow veins in a rabbit model of arteriovenous fistula. Abstract at Kidney Week, American Society of Nephrology; 2008. .

17. Hye RJ, Peden EK, O'Connor TP, Browne BJ, Dixon BS, Schanzer AS, et al. Human type I pancreatic elastase treatment of arteriovenous fistulas in patients with chronic kidney disease. J Vasc Surg 2014 Aug;60(2):454-61.

18. Strauss BH, Robinson R, Batchelor WB, Chisholm RJ, Ravi G, Natarajan MK, et al. In vivo collagen turnover following experimental balloon angioplasty injury and the role of matrix metalloproteinases. Circ Res 1996 Sep;79(3):541-50.

19. Owens GK, Kumar MS, Wamhoff BR. Molecular regulation of vascular smooth muscle cell differentiation in development and disease. Physiol Rev 2004 Jul;84(3):767-801.

20. Brooke BS, Bayes-Genis A, Li DY. New insights into elastin and vascular disease. Trends Cardiovasc Med 2003 Jul;13(5):176-81.

21. Ito S, Ishimaru S, Wilson SE. Inhibitory effect of type 1 collagen gel containing alpha-elastin on proliferation and migration of vascular smooth muscle and endothelial cells. Cardiovasc Surg 1997 Apr;5(2):176-83.

22. Ooyama T, Fukuda K, Oda H, Nakamura H, Hikita Y. Substratum-bound elastin peptide inhibits aortic smooth muscle cell migration in vitro. Arteriosclerosis 1987 Nov;7(6):593-8.

23. Roy-Chaudhury P, Arend L, Zhang J, Krishnamoorthy M, Wang Y, Banerjee R, et al. Neointimal hyperplasia in early arteriovenous fistula failure. Am J Kidney Dis 2007 Nov;50(5):782-90.

24. Li DY, Brooke B, Davis EC, Mecham RP, Sorensen LK, Boak BB, et al. Elastin is an essential determinant of arterial morphogenesis. Nature 1998 May 21;393(6682):276-80.

25. Misra S, Doherty MG, Woodrum D, Homburger J, Mandrekar JN, Elkouri S, et al. Adventitial remodeling with increased matrix metalloproteinase-2 activity in a porcine arteriovenous polytetrafluoroethylene grafts. Kidney Int 2005 Dec;68(6):2890-900.

26. Misra S, Shergill U, Yang B, Janardhanan R, Misra KD. Increased expression of HIF-1alpha, VEGF-A and its receptors, MMP-2, TIMP-1, and ADAMTS-1 at the venous stenosis of arteriovenous fistula in a mouse model with renal insufficiency. J Vasc Interv Radiol 2010 Aug;21(8):1255-61.

27. Rotmans JI, Velema E, Verhagen HJ, Blankensteijn JD, de Kleijn DP, Stroes ES, et al. Matrix metalloproteinase inhibition reduces intimal hyperplasia in a porcine arteriovenous-graft model. J Vasc Surg 2004 Feb;39(2):432-9.

28. Franano FN, Hance K, Bland KS, Burke SK. PRT-201 dilates outflow veins and improves maturation rates in a rabbit model of AVF. 22 ed. 2007.

29. Amabile PG, Wong H, Uy M, Boroumand S, Elkins CJ, Yuksel E, et al. In vivo vascular engineering of vein grafts: directed migration of smooth muscle cells by perivascular release of elastase limits neointimal proliferation. J Vasc Interv Radiol 2002 Jul;13(7):709-15.

30. Wong AH, Waugh JM, Amabile PG, Yuksel E, Dake MD. In vivo vascular engineering: directed migration of smooth muscle cells to limit neointima. Tissue Eng 2002 Apr;8(2):189-99.

31. Buus CL, Pourageaud F, Fazzi GE, Janssen G, Mulvany MJ, De Mey JG. Smooth muscle cell changes during flow-related remodeling of rat mesenteric resistance arteries. Circ Res 2001 Jul 20;89(2):180-6.

32. Cheung AK, Sarnak MJ, Yan G, Dwyer JT, Heyka RJ, Rocco MV, et al. Atherosclerotic cardiovascular disease risks in chronic hemodialysis patients. Kidney Int 2000 Jul;58(1):353-62.

33. Kennedy R, Case C, Fathi R, Johnson D, Isbel N, Marwick TH. Does renal failure cause an atherosclerotic milieu in patients with end-stage renal disease? Am J Med 2001 Feb 15;110(3):198-204.

34. Kokubo T, Ishikawa N, Uchida H, Chasnoff SE, Xie X, Mathew S, et al. CKD accelerates development of neointimal hyperplasia in arteriovenous fistulas. J Am Soc Nephrol 2009 Jun;20(6):1236-45.

Supplemental Data

Alpha smooth muscle actin staining

For the α-sma staining, deparaffinization and hydration of the 5 μm sections was followed by a treatment with 1% hydrogen peroxide and 5% bovine serum albumine in order to block the endogenous peroxidase and aspecific binding sites respectively. Incubation of the primary antibody was performed overnight at room temperature. Subsequently, sections were incubated at room temperature for 1 hour with HRP labelled antibodies against mouse IgG (Dako, Glostrup, Denmark) at 1:1000 dilution. Immunoreactive tissue was then developed by using a DAB peroxidase substrate kit (Dako, Glostrup, Denmark). Sections were counterstained with hematoxylin.